J Therm Anal Calorim (2016) 126:689–697
DOI 10.1007/s10973-016-5511-x

Mesophases of non-conventional liquid crystalline molecules

Short-chained alkyl-(F-alkyl)-alkyl semifluorinated alkanes—comparison with F-alkyl-(alkyl)-F-alkyl triblocks

Anna Chachaj-Brekiesz[1] · Natalia Górska[1] · Natalia Osiecka[2] · Patrycja Dynarowicz-Łątka[1]

Received: 4 February 2016 / Accepted: 27 April 2016 / Published online: 9 May 2016

Abstract Two homologous series of triblock molecules of the $H(CH_2)_n(CF_2)_6(CH_2)_nH$ and $F(CF_2)_n(CH_2)_6(CF_2)_nF$ general formulas with $n = 6$, 8, 10, and 12 have been synthesized and investigated using two complementary methods: differential scanning calorimetry and polarized optical microscopy in order to investigate their thermal behavior, establish phase diagram, and calculate thermodynamic parameters of the observed phase transitions. Although different from commonly known liquid crystal materials, all the compounds studied form thermotropic liquid crystalline phases (smectic or nematic) and undergo vitrification process.

Keywords Triblock semifluorinated alkanes · Liquid crystals · Mesophase · Thermal behavior · DSC · POM

Introduction

According to the classic approach, there are two main groups of molecules capable of forming liquid crystalline (LC) phases, i.e., anisometric and amphiphilic molecules. The former ones, of either rod- or disk-like shape, show thermotropic mesophases [1, 2]. On the other hand, amphiphilic molecules, built of two segments: polar and apolar, are known for forming lyotropic liquid crystalline mesophases. Semifluorinated alkanes (SFAs), consisting of hydrogenated and perfluorinated segments covalently bound within one molecule, are non-typical as regards conventional definition of liquid crystalline materials. Namely, although purely hydrophobic and rod-like shaped, their structure is not typically mesogenic since most of the mesogenic molecules have a rigid aromatic/cyclic frame (e.g., biphenyl, azobenzene, cyclopentanoperhydrophenanthrene) or multiple bonds extended in distal positions by long-chained alkyl substituents. Instead, SFAs possess a rigid fluorinated segment of helical conformation attached to flexible, zig-zag alkyl chains. Interestingly, although SFAs do not possess any polar group in their structure, they are amphiphilic and behave like surfactants as proved in Refs. [3, 4]. The simplest molecules of this kind are diblock semifluorinated alkanes of the $F(CF_2)_m(CH_2)_nH$ formula (in short F_mH_n). First molecule of this kind, for which liquid crystalline phase was observed, was $F_{10}H_{10}$ [5]. Further investigations revealed that—for majority of the investigated diblocks—the LC phase was classified as smectic B (see Refs. [6–8]), although for some homologs higher ordering (smectic G or J) was also identified.

Recently, we have synthesized a series of triblock SFAs of the $H(CH_2)_n(CF_2)_6(CH_2)_nH$ general formula (in short $H_nF_6H_n$) with $n = 12$, 14, 16, 18, and 20, which were found to exhibit thermotropic LC phases [9]. In this paper, we have extended our study to the $H_nF_6H_n$-type triblocks with shorter alkyl segments ($n = 6$, 8, and 10). The next homolog of this kind, i.e., with $n = 12$, has already been investigated; however, for the sake of comparison, the results adopted from Ref. [9] are also shown here. Additionally, we have synthesized and investigated triblocks of different structures, i.e., with an alkyl fragment extended in distal positions by two fluorinated segments, i.e., $F(CF_2)_n(CH_2)_6(CF_2)_nF$ (in short $F_nH_6F_n$) with $n = 6$, 8, 10, and 12, and performed a comparative study of both kinds of triblocks.

✉ Patrycja Dynarowicz-Łątka
ucdynaro@cyf-kr.edu.pl

[1] Faculty of Chemistry, Jagiellonian University, Ingardena 3, 30-060 Kraków, Poland

[2] The Henryk Niewodniczański Institute of Nuclear Physics, Polish Academy of Sciences, Radzikowskiego 152, 31-342 Kraków, Poland

Experimental

Materials

Synthesis of semifluorinated triblock molecules

Homologs from $F_nH_6F_n$ and $H_nF_6H_n$ series were synthesized following experimental conditions, which were previously described by Twieg and Rabolt [10] (for $F_mH_nF_m$ compounds) as well as applied in our former paper [9] (for $H_nF_mH_n$ compounds). Composition and purity of the synthesized triblocks were confirmed by elemental analysis. Additionally, nuclear magnetic resonance spectra were recorded for $H_nF_6H_n$ compounds, which were soluble in standard laboratory solvents in contrast to $F_mH_6F_m$ series. Analytical data of the synthesized compounds are as follows:

1,1,1,2,2,3,3,4,4,5,5,6,6,13,13,14,14,15,15,16,16,17,17,18,18,18-hexacosafluorooctadecane (**$F_6H_6F_6$**): composition measured: C 30.14 % H 1.89 % (calculated: C 29.93 % H 1.67 % F 68.39 %);

1,1,1,2,2,3,3,4,4,5,5,6,6,7,7,8,8,15,15,16,16,17,17,18,18,19,19,20,20,21,21,22,22,22-tetratriacontafluorodocosane (**$F_8H_6F_8$**): composition measured: C 28.75 % H 1.38 % (calculated: C 28.65 % H 1.31 % F 70.04 %);

1,1,1,2,2,3,3,4,4,5,5,6,6,7,7,8,8,9,9,10,10,17,17,18,18,19,19,20,20,21,21,22,22,23,23,24,24,25,25,26,26,26-dotetracontafluorohexacosane (**$F_{10}H_6F_{10}$**): composition measured: C 28.00 % H 1.11 % (calculated: C 27.82 % H 1.08 % F 71.10 %);

1,1,1,2,2,3,3,4,4,5,5,6,6,7,7,8,8,9,9,10,10,11,11,12,12,19,19,20,20,21,21,22,22,23,23,24,24,25,25,26,26,27,27,28,28,29,29,30,30,30-pentacontafluorotriacontane (**$F_{12}H_6F_{12}$**): composition measured: C 26.94 % H 0.97 % (calculated: C 27.25 % H 0.91 % F 71.84 %);

7,7,8,8,9,9,10,10,11,11,12,12-dodecafluorooctadecane (**$H_6F_6H_6$**): ^{1}H NMR (300 MHz, $CDCl_3$) δ 2.16–1.93 (m, 4H), 1.66–1.53 (m, 4H), 1.45–1.20 (m, 20H), 0.89 (*t*, $J = 6.8$ Hz, 6H); composition measured: C 45.81 % H 5.50 % (calculated: C 45.96 % H 5.57 % F 48.47 %);

9,9,10,10,11,11,12,12,13,13,14,14-dodecafluorodocosane (**$H_8F_6H_8$**): ^{1}H NMR (300 MHz, $CDCl_3$) δ 2.16–1.93 (m, 4H), 1.67–1.54 (m, 4H), 1.46–1.25 (m, 12H), 0.90 (*t*, $J = 6.8$ Hz, 6H); composition measured: C 49.90 % H 6.45 % (calculated: C 50.19 % H 6.51 % F 43.30 %)

11,11,12,12,13,13,14,14,15,15,16,16-dodecafluorohexacosane (**$H_{10}F_6H_{10}$**): ^{1}H NMR (300 MHz, $CDCl_3$) δ 2.16–1.92 (m, 4H), 1.66–1.50 (m, 4H), 1.42–1.24 (m, 28H), 0.89 (*t*, $J = 6.6$ Hz, 6H); composition measured: C 53.44 % H 7.17 % (calculated: C 53.60 % H 7.27 % F 39.13 %);

13,13,14,14,15,15,16,16,17,17,18,18-dodecafluorotriacontane (**$H_{12}F_6H_{12}$**): ^{1}H NMR (300 MHz, $CDCl_3$) δ 2.16–1.93 (m, 4H), 1.67–1.52 (m, 4H), 1.44–1.20 (m, 36H), 0.88 (*t*, $J = 6.7$ Hz, 6H); composition measured: C 56.79 % H 7.84 % (calculated: C 56.41 % H 7.89 % F 35.69 %).

Methods

Differential scanning calorimetry

DSC measurements were performed for the two series of triblocks, $H_nF_6H_n$ and $F_nH_6F_n$, using Mettler-Toledo 821^e and 822^e calorimeters in the temperature range of 150–410 K with the scanning rates of 10, 5, and 2 K min^{-1}. The masses of the $H_nF_6H_n$ bulk samples with $n = 6$, 8, 10, and 12 were equal to 13.07, 4.35, 2.76, and 6.93 mg, respectively. The masses of the $F_nH_6F_n$ bulk samples with $n = 6$, 8, 10, and 12 were equal to 6.78, 3.93, 3.34, and 4.19 mg, respectively. The samples were placed in hermetically sealed aluminum pans (30 μL). The instrument was calibrated using the literature data for indium and ice melting points. The enthalpy changes (ΔH) linked up with observed transitions were calculated by numerical integration of the DSC curves under the peaks of the anomalies. The estimations of entropy changes (ΔS) were calculated using the following formula: $\Delta S = \Delta H/T_C$. The transition temperatures T_C were considered to be the peak temperatures (T_{peak}) from the DSC curves obtained on heating and cooling. The transition temperatures are given with accuracy of ±0.5 K. The values of the enthalpy and entropy changes at the transitions are given with the accuracy of about 20 %.

Polarized optical microscopy

The textures of different phases observed were identified using Biolar PI polarized microscope (PZO Warsaw). The temperature was stabilized by Linkam THM 600 silver heating/cooling stage and TMS 90 temperature controller. Transition temperatures were measured by platinum resistance thermometer stabilized with temperature accuracy of ±0.1 K. The observations were carried out both during heating and cooling in the temperature range of 170–420 K.

Results and discussion

Studies of polymorphism of all the investigated homologous substances of two types of semifluorinated triblock molecules were carried out using two complementary experimental methods: differential scanning calorimetry (DSC) and texture observations with the polarized optical microscopy (POM). Results of the performed measure-

ments let us verify if the investigated compounds form ordered solid, plastic, liquid crystalline or vitreous phases and characterize them by estimation of thermodynamic parameters, such as transition temperature, enthalpy, and entropy changes at the transitions. All the DSC curves were obtained for virgin samples, both during heating and subsequent cooling, and registered with a scanning rate of 10 K min^{-1}. For clarification of some of our results, we have performed additional DSC measurements with smaller scanning rates (5 or 2 K min^{-1}). Also, all the images of textures shown herein were recorded for bulk samples with the rates of 10 or 5 K min^{-1}.

$H_nF_6H_n$ homologs

The $H_6F_6H_6$ compound is the only one investigated in this work which is isotropic liquid at room temperature. Based on POM observations, it undergoes three phase transitions. Two of them, observed consecutively in the DSC curve during heating at $T_{C2} = 200.5$ K and $T_{C1} = 242.1$ K, occur in the solid state. The first one at T_{C2} is connected with the transition between glass state and LC smectic phase (GSmX → SmX). From texture observation, we could not establish what type of smectic phase it is. However, due to the anticipated theoretical sequence of LC thermotropic mesophases, it can be either smectic K or smectic H phase. The second transition at T_{C1} occurs between two LC smectic phases (SmX → SmE). The third transition at $T_{Iso} = 294.2$ K is associated with conversion into isotropic liquid (SmE → Iso). Interestingly, there is also one small and broad anomaly with a maximum observed at 274 K (on heating) and 270 K (on cooling) in both DSC curves (see Fig. 1). However, the existence of additional phase corresponding to this anomaly in this temperature region was not confirmed by optical

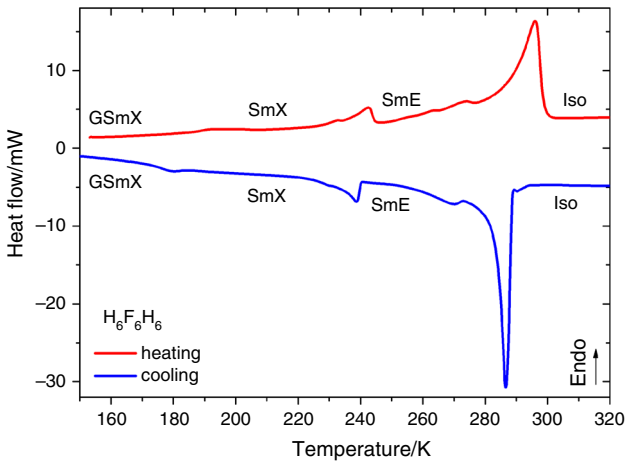

Fig. 1 DSC curves of $H_6F_6H_6$ presented between 150 and 320 K registered with a scanning rate of 10 K min^{-1}

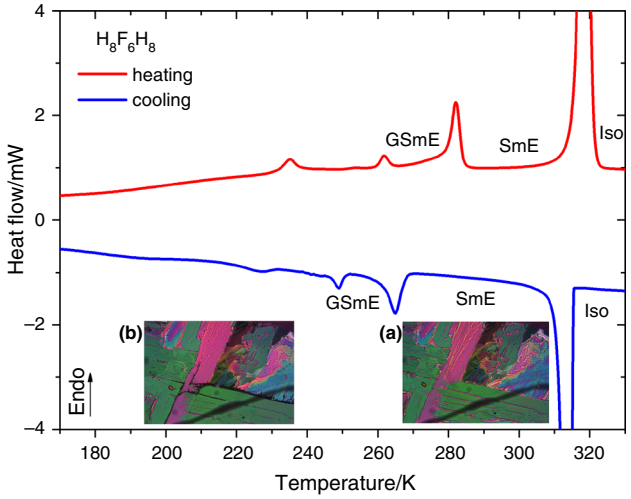

Fig. 3 DSC curves of $H_8F_6H_8$ presented between 170 and 330 K registered with a scanning rate of 10 K min^{-1} together with textures of **a** SmE phase ($T = 303$ K) and **b** GSmE phase ($T = 264$ K) both observed upon cooling

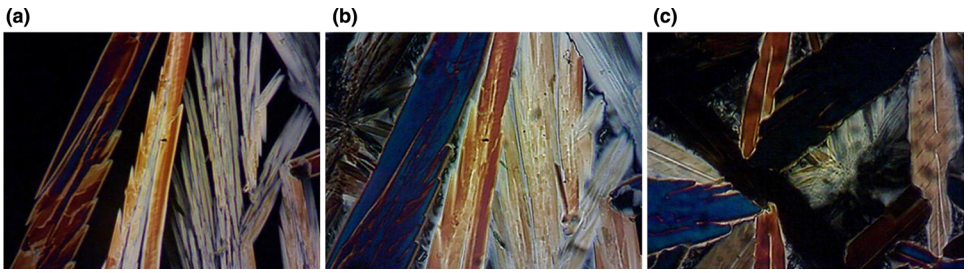

Fig. 2 Textures of $H_6F_6H_6$ phases: **a** SmE phase ($T = 284$ K), **b** SmX (SmK or SmH) ($T = 224$ K), and **c** GSmX (GSmK or GSmH) phase ($T = 174$ K) observed upon cooling

microscopy. Images of the observed phases are presented in Fig. 2.

Taking into consideration the results obtained using the two methods, the following phase sequence could be established: Iso $\overset{286K}{\longrightarrow}$ SmE $\overset{239K}{\longrightarrow}$ SmX $\overset{181K}{\longrightarrow}$ GSmX.

Figure 3 presents the DSC curves obtained for the $H_8F_6H_8$ homolog together with POM images of smectic E (SmE) phase with characteristic mosaic texture and glass of smectic E (GSmE) phase. There are four anomalies visible both during heating and cooling. Phase identification based on texture observation let us determine that the high-temperature large and sharp anomaly observed during heating at $T_{Iso} = 318.5$ K is connected with isotropization process, whereas the other three low-temperature anomalies visible in the DSC curves below 290 K are connected with three-step transition between LC smectic phase (SmE) and glass phase (SmE ↔ GSmE). The polarized optical microscopy observation of the steadily cooled sample complemented with DSC results led to the following phase sequence: Iso $\overset{314K}{\longrightarrow}$ SmE $\overset{265K,249K,227K}{\longrightarrow}$ GSmE

The DSC results obtained for the $H_{10}F_6H_{10}$ homolog are presented in Fig. 4. Two endothermic anomalies can be distinguished in the DSC curve registered during heating with a scanning rate of 10 K min^{-1}, one small with a maximum at $T_{C2} = 294.8$ K and another large and very broad with a maximum at $T_{C1} = 319.9$ K. Based on POM observation, it could be established that the first anomaly is connected with the transition between two plastic crystal phases (PCrII → PCrI) and the second anomaly is connected with the transition between plastic crystal and nematic phases (PCrI → N). The isotropization process can be visible in the DSC curve after applying smaller scanning rate (see DSC curve obtained upon heating with 2 K min^{-1} in Fig. 4). The Iso → N and N → PCrI transitions are clearly visible in the DSC curves registered upon cooling with both scanning rates. In turn, the

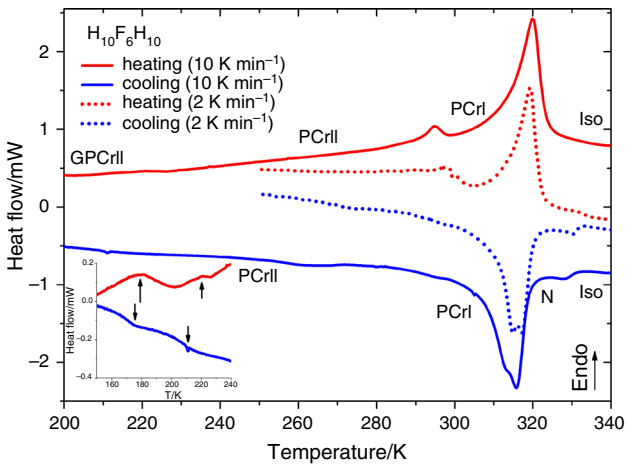

Fig. 4 A comparison of the DSC curves of $H_{10}F_6H_{10}$ registered with two scanning rates: 10 and 2 K min^{-1}

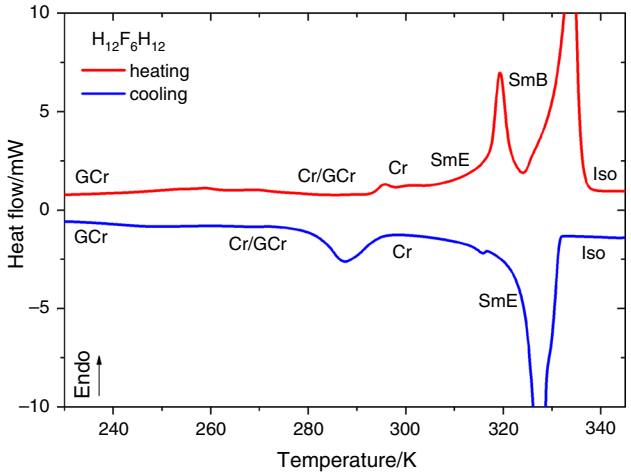

Fig. 6 DSC curves of $H_{12}F_6H_{12}$ presented between 230 and 345 K registered with a scanning rate of 10 K min^{-1} [9]

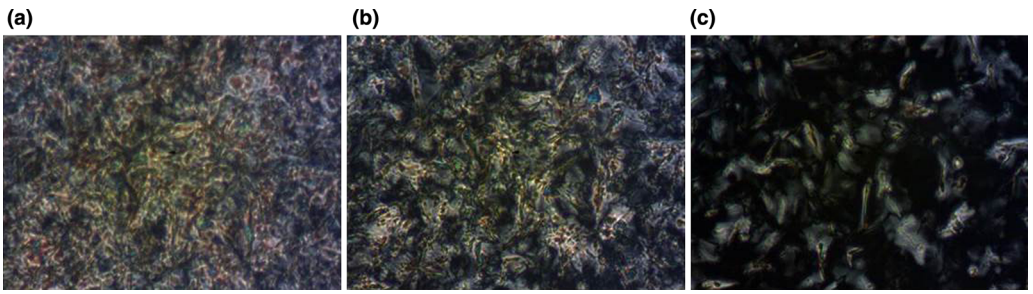

Fig. 5 Textures of $H_{10}F_6H_{10}$ phases: **a** PCrII phase ($T = 291$ K), **b** PCrI phase ($T = 321$ K), and **c** nematic phase ($T = 324$ K) observed upon heating

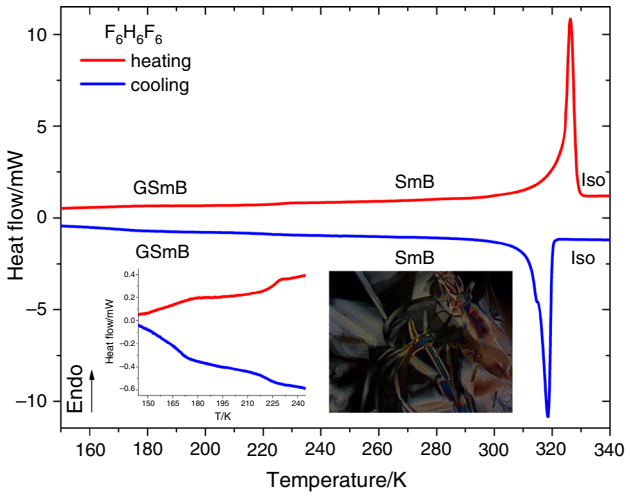

Fig. 7 DSC curves of $F_6H_6F_6$ together with texture of smectic B phase ($T = 298$ K) observed upon cooling with a rate of 10 K min^{-1}. *Inset*: magnification of the DSC curve obtained between 144 and 245 K

transition from PCrI to PCrII is poorly stressed in the DSC curve during cooling—small peak at 296 K can be connected with this transition. The transition from PCrI to PCrII was not observed with optical microscopy. Textures of both plastic crystal phases and nematic phase observed upon heating are presented in Fig. 5. Additionally, very broad and small anomalies can be also visible after magnification at about 220 and 179 K during heating, and at about 263, 211, and 175 K during cooling in the DSC curves (see inset to Fig. 4). This is most probably connected with gradual vitrification of plastic crystal phase (PCrII). However, the cracks on the plastic crystal texture were not observed. Taking into consideration the DSC and POM results, the following phase sequence can be established: $\text{Iso} \xrightarrow{328K} \text{N} \xrightarrow{316K} \text{PCrI} \xrightarrow{296K} \text{PCrII} \xrightarrow{263K,211K,175K} \text{GPCrII}$.

Figure 6 presents the DSC diagram obtained for the last homolog investigated in this group, i.e., $H_{12}F_6H_{12}$. The DSC and POM results have been already presented in our

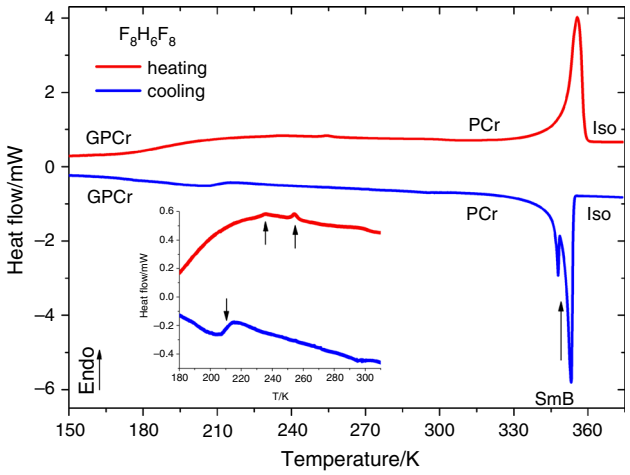

Fig. 8 DSC curves of $F_8H_6F_8$ presented between 150 and 375 K registered with a scanning rate of 10 K min^{-1}. *Inset*: magnification of the DSC curves between 180 and 310 K

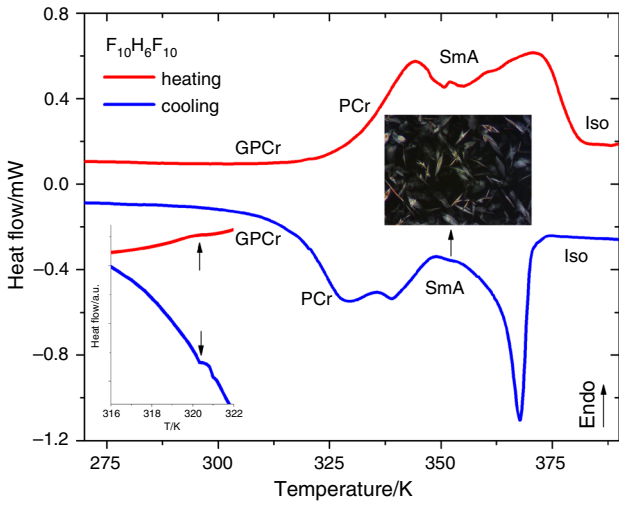

Fig. 10 DSC curves of $F_{10}H_6F_{10}$ presented between 270 and 390 K registered with a scanning rate of 10 K min^{-1} together with texture of SmA phase ($T = 361$ K) [11]

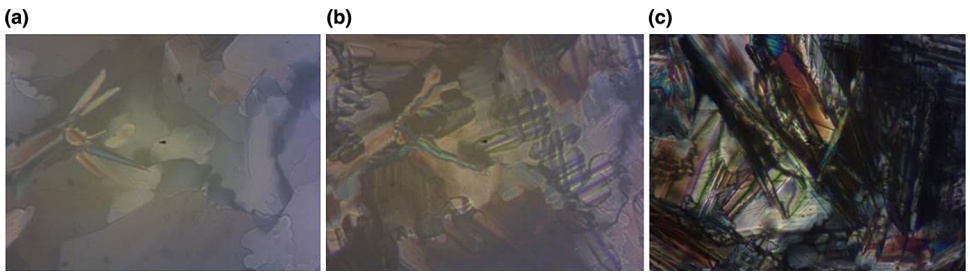

Fig. 9 Textures of $F_8H_6F_8$ phases: **a** SmB phase ($T = 349$ K), **b** PCr phase ($T = 316$ K), and **c** GPCr ($T = 200$ K) observed upon cooling

previous paper [9]. The compound exhibits two LC phases, smectic B and E, and one crystal phase, which gradually undergoes vitrification process below 300 K.

$F_nH_6F_n$ homologs

The DSC curves obtained for $F_6H_6F_6$ are presented in Fig. 7. In temperatures between 240 and 340 K, one large and sharp anomaly can be observed during heating with a maximum at $T_{Iso} = 326$ K and one large exothermic anomaly with a maximum at $T_{cryst} = 319$ K with a shoulder visible at about 314.5 K during cooling process. Based on the texture observation, the anomalies observed during heating and cooling are connected with conversion of the LC smectic B (SmB) phase into isotropic liquid and crystallization process, respectively. Although there is an exothermic shoulder visible in the DSC curve during cooling, upon further cooling the image of texture did not change, even below 220 K. This behavior suggests that glass of SmB phase is formed in low temperatures. The temperature of the transition to the glass phase of SmB was not possible to be established from POM measurements, as cracks on the texture were not observed. Except for high-temperature anomaly, the DSC curve obtained during cooling shows two deflections at about 221 and 162 K, which indicates—most probably—a gradual vitrification process. During subsequent heating, two deflections are visible at about 164 and 223 K in the DSC curve (see inset of Fig. 7).

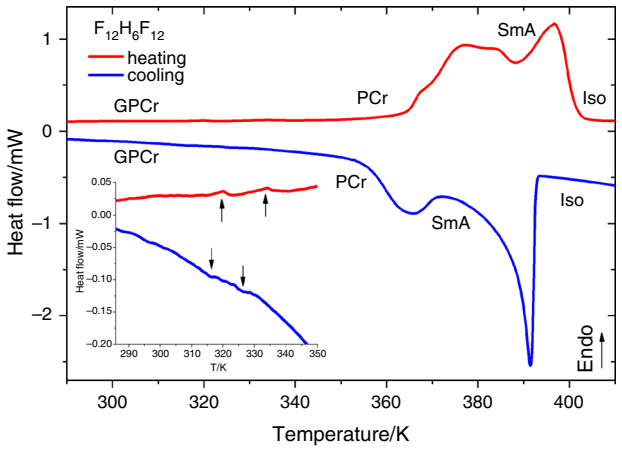

Fig. 11 DSC curves of $F_{12}H_6F_{12}$ presented between 290 and 410 K registered with a scanning rate of 10 K min^{-1}

Based on the discussed results, the phase sequence is as follows: Iso $\xrightarrow{319K}$ SmB $\xrightarrow{221K,162K}$ GSmB.

The $F_8H_6F_8$ homolog also exhibits one mesophase, smectic B (SmB) phase, and one plastic crystal phase. Based on the optical microscopy observation of the steadily cooled sample and DSC results, the following phase sequence occurs: Iso $\xrightarrow{353K}$ SmB $\xrightarrow{348K}$ PCr $\xrightarrow{211K}$ GPCr.

During cooling of the sample from isotropic liquid (Iso), the Iso → SmB phase transition is observed in DSC curve at 353 K (see Fig. 8). The characteristic mosaic texture of SmB phase was registered for this compound at 349 K, which is shown in Fig. 9a. The rate of the SmB–PCr transition is very fast. During cooling, this transition occurs in the DSC curve at $T_{C1} = 348$ K. During heating, only the SmB → Iso transition is observed in the DSC curve at $T_{Iso} = 356$ K, even for larger scanning rates applied. One

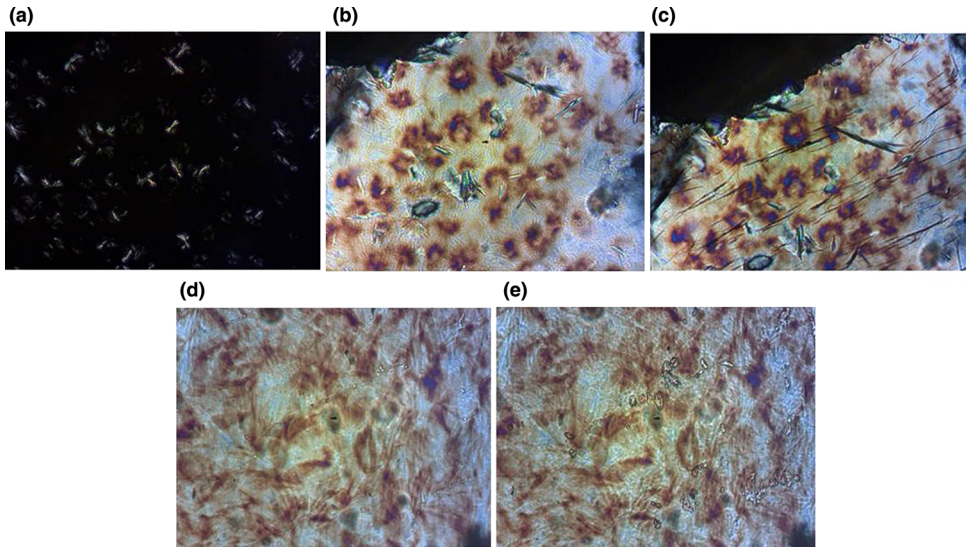

Fig. 12 Textures of $F_{12}H_6F_{12}$ phases: **a** SmA phase ($T = 398$ K), **b** PCr phase ($T = 383$ K), **c** GPCr phase ($T = 283$ K) observed upon cooling with the rate of 10 K min^{-1} and **d** GPCr phase ($T = 240$ K), **e** GPCr phase ($T = 248$ K) observed upon heating with a rate of 5 K min^{-1}

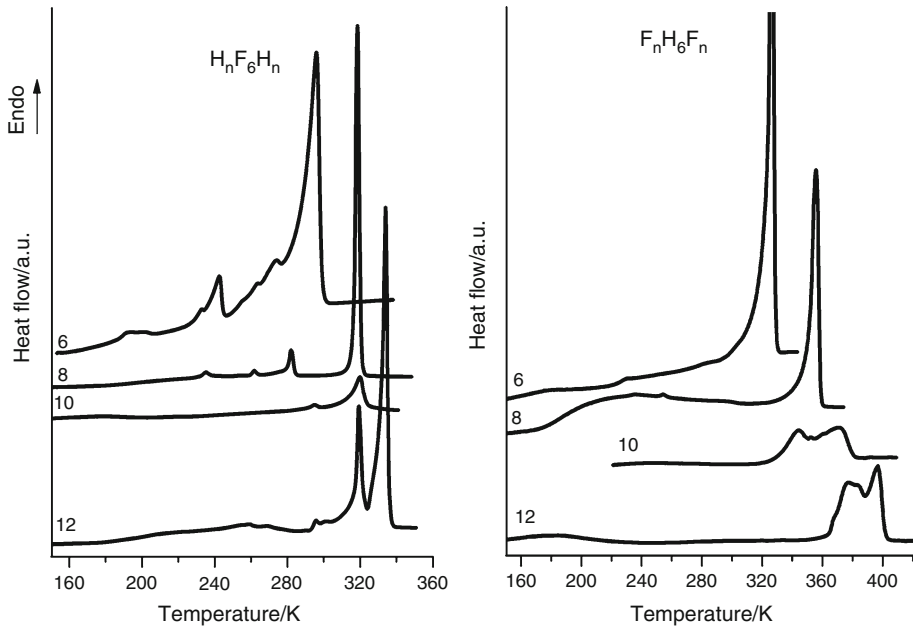

Fig. 13 A comparison of the DSC curves obtained for the $H_nF_6H_n$ and $F_nH_6F_n$ samples ($n = 6$, 8, 10, and 12) during heating with a scanning rate of 10 K min^{-1}

plastic crystal phase was discovered by the microscopy observations as no other textures were revealed. The conversion to glass phase was manifested by rapid appearance of cracks in the PCr texture at 212 K. The cracks disappeared at 278 K. The results of texture observations and DSC are in a good agreement. The transition into glass phase PCr → GPCr is visible in the DSC curve at 211 K (blue lower curve in the inset to Fig. 8), and the transition into plastic crystal phase GPCr → PCr appeared at 236 and 254 K (red upper curve in the inset of Fig. 8).

Figure 10 presents DSC curves obtained for $F_{10}H_6F_{10}$ between 270 and 390 K. The DSC and POM results have been already presented in our previous paper [11]. The investigated compound exhibits at least four different phases in the following sequence during cooling procedure: $\text{Iso} \xrightarrow{368K} \text{SmA} \xrightarrow{339K} \text{PCr} \xrightarrow{320K} \text{GPCr}$. DSC results suggest existence of one more distinguishable phase between 339 and 329 K (upon cooling), but it was not confirmed by optical microscopy—images of the textures recorded between 339 and 321 K were the same.

The DSC curves obtained for $F_{12}H_6F_{12}$ between 290 and 410 K and corresponding textures of the observed phases are presented in Figs. 11 and 12, respectively. The temperatures obtained with POM method are shifted significantly toward higher temperatures as compared to the DSC results. During heating, the transitions GPCr → PCr, PCr → SmA, and SmA → Iso were observed at 364, 409, and 412 K, respectively. In turn, during cooling, the transitions Iso → SmA, SmA → PCr, and PCr → GPCr were observed at 400, 397, and 334 K, respectively. Interestingly, during heating with a rate of 5 K min^{-1}, the crystal nucleation appeared in the GPCr texture at 240 K visible as

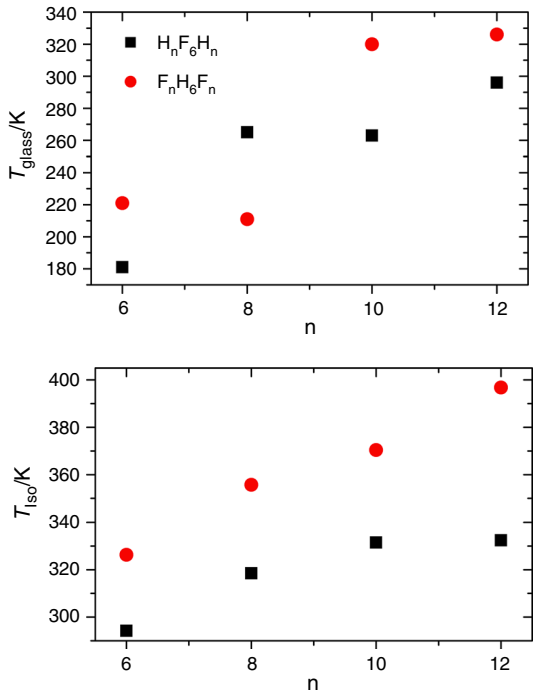

Fig. 14 Glass and isotropization temperatures of the $H_nF_6H_n$ and $F_nH_6F_n$ samples based on the DSC results

small spots in the texture in Fig. 12d. These spots keep growing till 250 K (see Fig. 12e) and then melt. With a rate higher than 5 K min^{-1}, this phenomenon is not observed as the crystallization rate is low. The phase sequence in this compound: $\text{Iso} \xrightarrow{391K} \text{SmA} \xrightarrow{366K} \text{PCr} \xrightarrow{326K,316K} \text{GPCr}$ is basically the same as that observed for the $F_{10}H_6F_{10}$ homolog, except for the transitions appearing at higher temperature.

Table 1 Thermodynamic parameters of the detected phase transitions for the $H_nF_6H_n$ and $F_nH_6F_n$ series ($n = 6$–12) obtained by DSC in comparison with the phase transition temperatures observed by POM

Substance	Transition type	T_C/K DSC	T_C/K POM	$\overline{\Delta H}$/ kJ mol^{-1}	$\overline{\Delta S}$/ J mol^{-1} K^{-1}	Transition type	T_C/K DSC	T_C/K POM	$\overline{\Delta H}$/ kJ mol^{-1}	$\overline{\Delta S}$/ J mol^{-1} K^{-1}
$H_nF_6H_n$	Heating					Cooling				
$H_6F_6H_6$	GSmX → SmX	200.5	219.8	0.7	3.5	SmX → GSmX	181.0	200.8	1.4	7.7
	SmX → SmE	242.1	249.8	2.3	9.5	SmE → SmX	238.7	234.8	2.5	10.5
	SmE → Iso	294.2	298.1	10.9	37.0	Iso → SmE	286.1	292.3	12.5	43.7
$H_8F_6H_8$	GSmE → SmE	235.2	–	–	–	SmE → GSmE	227.0	–	–	–
	GSmE → SmE	261.8	–	–	–	SmE → GSmE	249.0	–	–	–
	GSmE → SmE	282.1	288.3	–	–	SmE → GSmE	265.0	279.5	–	–
	SmE → Iso	318.5	318.6	35.6	111.8	Iso → SmE	314.4	315.8	35.2	112.0
$H_{10}F_6H_{10}$	GPCrII → PCrII	~179	–	–	–	PCrII → GPCrII	~175	–	–	–
	GPCrII → PCrII	~220	–	–	–	PCrII → GPCrII	~211	–	–	–
	–	–	–	–	–	PCrII → GPCrII	~263	–	–	–
	PCrII → PCrI	294.8	303.6	1.1	3.7	PCrI → PCrII	~296	–	–	–
	PCrI → N	319.9	322.8	16.9	52.8	N → PCrI	315.7	315.5	16.8	53.2
	N → Iso	331.5	334.8	–	–	Iso → N	328.2	325.1	0.3	0.9
$H_{12}F_6H_{12}$	GCr → Cr	~260	–	–	–	Cr → GCr	~250	–	–	–
	GCr → Cr	300.2	299.8	–	–	Cr → GCr	296.0	309.9	–	–
	Cr → SmE	–	–	–	–	SmE → Cr	316.2	316.3	–	–
	SmE → SmB	318.1	–	17.0	53.0	SmB → SmE	329.8	330.2	12.0	41.0
	SmB → Iso	332.4	336.2	39.0	117.0	Iso → SmB	330.6	332.7	42.0	127.0
$F_nH_6F_n$										
$F_6H_6F_6$	GSmB → SmB	~164	–	–	–	SmB → GSmB	~162	–	–	–
	GSmB → SmB	~223	–	–	–	SmB → GSmB	~221	–	–	–
	SmB → Iso	326.3	328.5	30.4	93.2	Iso → SmB	318.6	319.9	29.1	91.3
$F_8H_6F_8$	GPCr → PCr	~236	–	–	–					
	GPCr → PCr	~254	278.0	–	–	PCr → GPCr	~211	212.0	–	–
	PCr → SmB	–	356.9	–	–	SmB → PCr	347.9	348.5	–	–
	SmB → Iso	355.7	358.9	33.2[a]	93.3[a]	Iso → SmB	353.2	355.6	33.1[a]	93.7[a]
$F_{10}H_6F_{10}$	GPCr → PCr	~320	324.6	–	–	PCr → GPCr	~320	323.9	–	–
	PCr → SmA	344.4	356.6	–	–	SmA → PCr	338.9	342.5	–	–
	SmA → Iso	370.4	379.3	31.4[a]	84.8[a]	Iso → SmA	367.9	373.0	30.8[a]	83.7[a]
$F_{12}H_6F_{12}$	GPCr → PCr	320.1	–	–	–	PCr → GPCr	~316	–	–	–
	GPCr → PCr	334.1	364.0	–	–	PCr → GPCr	~326	333.7	–	–
	PCr → SmA	377.2	408.8	–	–	SmA → PCr	365.8	397.3	–	–
	SmA → Iso	396.8	411.6	46.6[a]	117.5[a]	Iso → SmA	391.4	399.7	39.9[a]	101.9[a]

[a] The combined value calculated for both high-temperature anomalies

Following acronyms were used: *Iso* isotropic liquid, *N* nematic, *SmA* smectic A, *SmB* smectic B, *SmE* smectic E, *SmX* smectic K or H, *GSmB* glass of SmB, *GSmE* glass of SmE, *PCr* plastic crystal, *GPCr* glass of PCr, *Cr* crystal, *GCr* glass of crystal

Figure 13 summarizes the calorimetric results obtained during heating, while Fig. 14 shows glass and isotropization temperatures for both series of the investigated homologs, $H_nF_6H_n$ and $F_nH_6F_n$. The thermodynamic parameters of the detected phase transitions, such as transition temperatures T_C and enthalpy and entropy changes, ΔH and ΔS, based on the DSC results, are compiled in Table 1.

Conclusions

Two series of triblock molecules consisting of hydrogenated and perfluorinated building blocks, located either in the middle or at the end of molecules, differing in the length of terminal segments have been synthesized. The performed experiments, involving DSC and POM, allowed us to draw the following conclusions:

- All the investigated $H_nF_6H_n$ and $F_nH_6F_n$ triblock molecules form thermotropic liquid crystalline phases (smectic or nematic). One LC phase of smectic ordering (SmA or SmB) was observed for all the studied four homologs of the $F_nH_6F_n$ type. Among the $H_nF_6H_n$ homologs, one smectic (SmE) phase and one nematic phase were observed in $H_8F_6H_8$ and $H_{10}F_6H_{10}$, respectively. The other two compounds in this series, i.e., $H_6F_6H_6$ and $H_{12}F_6H_{12}$, exhibit two smectic phases.
- For both $H_nF_6H_n$ and $F_nH_6F_n$ series, it can be observed that the longer hydrocarbon or perfluorinated segments extended in distal positions, the higher temperature of the transition into isotropic liquid (Sm or N → Iso). Isotropization temperatures observed for the $F_nH_6F_n$ series are significantly higher than those for $H_nF_6H_n$.
- All the studied compounds from both series ($H_nF_6H_n$ and $F_nH_6F_n$) undergo vitrification process, which—for the majority of the homologs under investigation—proceeds gradually. Generally, the glass temperature is higher for compounds with longer hydrocarbon or fluorinated segments extended in distal positions.
- One crystalline phase, most probably plastic one, has been observed in all the compounds from $F_nH_6F_n$ series, except for $F_6H_6F_6$. Among the $H_nF_6H_n$ homologs studied in this work, only $H_{10}F_6H_{10}$ exhibited plastic crystal phases.
- No metastable behavior was observed in any of the studied compounds.
- Analyzing the results obtained for the previously studied compounds of the $H_nF_6H_n$ type with even number of n = 12, 14, 16, 18, and 20 [9], it can be concluded that molecules with n between 20 and 12 exhibit two LC phases, SmE and SmB (except for $H_{14}F_6H_{14}$ where three LC phases were observed: SmE, SmB, and SmA). The $H_nF_6H_n$ compounds with n = 10 and 8, namely $H_{10}F_6H_{10}$ and $H_8F_6H_8$, show one LC phase, nematic and SmE, respectively. Interestingly, the homolog with the shortest hydrocarbon segments extended in distal positions studied so far—$H_6F_6H_6$—exhibits two LC smectic phases.

References

1. Demus D, Goodby JW, Gray GW, Spiess HW, Vill V. Handbook of liquid crystals. Weinheim: Wiley-VCH; 1998.
2. Ramamoorthy A, editor. Thermotropic liquid crystals: recent Advances. New York: Springer; 2007.
3. Turberg MP, Brady JE. Semifluorinated hydrocarbons: primitive surfactant molecules. J Am Chem Soc. 1988;110:7797–801.
4. Gaines GL. Surface activity of semifluorinated alkanes: $F(CF_2)_m(CH_2)_nH$. Langmuir. 1991;7:3054–6.
5. Mahler W, Guillon D, Skoulios A. Smectic liquid crystal from (perfluorodecyl)decane. Mol Cryst Liq Cryst Lett. 1985;2:111–9.
6. Broniatowski M, Dynarowicz-Łątka P, Witko W. Critical influence of the alkane length in surface and liquid-crystalline properties of perfluorodecyl-n-alkanes. J Fluor Chem. 2005;126:79–86.
7. Krafft MP, Riess JG. Chemistry, physical chemistry, and uses of molecular fluorocarbon-hydrocarbon diblocks, triblocks, and related compounds—unique "apolar" components for self-assembled colloid and interface engineering. Chem Rev. 2009;109:1714–92.
8. Tschierske C, editor. Liquid crystals: materials design and assembly. Topics in current chemistry, vol. 318. New York: Springer; 2012. p. 1–109.
9. Chachaj-Brekiesz A, Górska N, Osiecka N, Mikuli E, Dynarowicz-Łątka P. Synthesis and thermal behaviour of triblock semifluorinated n-alkanes. J Therm Anal Calorim. 2016;124:251–60.
10. Twieg RJ, Rabolt JF. Structural studies of semifluorinated n-alkanes. 3. Synthesis and characterization of $F(CF_2)_n(CH_2)_m(CF_2)_nF$. Macromolecules. 1988;21:1806–11.
11. Chachaj-Brekiesz A, Górska N, Osiecka N, Makyła-Juzak K, Dynarowicz-Łątka P. Surface and liquid-crystalline properties of $F_mH_nF_m$ triblock semifluorinated n-alkanes. Mater Sci Eng C. 2016;62:870–8.